

Article

Optimizing Solar Heating for Thangka Exhibition Halls: A Case Study in Malkang Cultural Village

Wenyang Han, Yan Bai, Miao Du, Yujie Tao, Yin Zhang *  and Qianru Yang *

School of Architecture, Southwest Minzu University, Chengdu 610225, China; 230813002016@stu.swun.edu.cn (W.H.); 202131701002@stu.swun.edu.cn (Y.B.); 13292316719@163.com (M.D.); t18807926746@163.com (Y.T.)

* Correspondence: cdzhangyin@163.com (Y.Z.); yangqianru@swun.edu.cn (Q.Y.); Tel.: +86-134-8891-8589 (Y.Z.); +86-156-8001-6301 (Q.Y.)

Abstract: With the continuous development of rural revitalization and urbanization in China, the sustainable transformation of traditional rural architecture has become increasingly important. This study takes the Thangka exhibition hall in rural Malkang, Sichuan Province, as the research object and proposes a Thangka exhibition hall architectural design centered around solar heating and aiming for near-zero energy consumption. The research method involves establishing a solar energy system model on the roof of the exhibition hall and utilizing solar angle and area calculation formulas along with simulation software to calculate the optimal installation angle and area of solar panels, with the aim of achieving indoor temperatures that meet Thangka protection requirements while achieving zero-energy heating. Preliminary results indicate that this solar-centric near-zero energy architectural design can effectively promote the increase in indoor temperature through solar thermal conversion. Additionally, through calculation and simulation, the optimal installation angle for the solar panels achieving zero-energy heating is determined to be 24.25 with an azimuth angle of -1.2 . The optimum installation area for solar panels is 8.2 square meters in the showroom and 2.7 square meters in the storeroom. Among these, the solar panel area for the Thangka exhibition hall constitutes 4.12% of the total area and is required for maintaining Thangka protection temperature requirements throughout the year, while the solar panel area for the storage room constitutes 1.88% and is also needed for the same purpose. Studying the optimal installation angle and area of solar panels can transform the exhibition hall into a near-zero-energy building, meeting the temperature requirements for Thangka preservation and human thermal comfort, while also achieving optimal economic benefits. This provides guidance and a reference for promoting near-zero-energy buildings in rural areas.

Keywords: rural architecture; solar radiation; Thangka exhibition hall; building optimization; thermal economy



Citation: Han, W.; Bai, Y.; Du, M.; Tao, Y.; Zhang, Y.; Yang, Q. Optimizing Solar Heating for Thangka Exhibition Halls: A Case Study in Malkang Cultural Village. *Energies* **2024**, *17*, 2091. <https://doi.org/10.3390/en17092091>

Academic Editor: Tullio De Rubeis

Received: 30 March 2024

Revised: 19 April 2024

Accepted: 25 April 2024

Published: 27 April 2024



Copyright: © 2024 by the authors. Licensee MDPI, Basel, Switzerland. This article is an open access article distributed under the terms and conditions of the Creative Commons Attribution (CC BY) license (<https://creativecommons.org/licenses/by/4.0/>).

1. Introduction

With the deepening of sustainable development concepts, the issue of pollution from traditional energy sources in buildings has attracted increasing attention. China is currently at a critical juncture in the development of renewable energy, with more and more renewable energy projects being implemented in western China, indicating the nation's emphasis on renewable energy. Thangka, as an important protected cultural relic in China, has also received increasing attention in recent years. How to properly protect and utilize Thangka under the conditions of sustainable development has become an important research direction in current Thangka preservation efforts.

Solar heating technology has been a focus of research due to its potential for effectively utilizing renewable energy for heating purposes. Researchers have explored various innovative methods to enhance the performance of solar heating systems and improve energy efficiency. Some researchers have conducted studies based on practical considerations. Fei et al. (2022) introduced a novel switchable surface coating that can quickly transition

between high solar reflectance and high solar energy transmission, enabling passive radiative cooling and solar heating to be achieved on a single platform [1]. Dai et al. (2022) developed a Janus film with the capability of radiative cooling and solar heating, providing a dual-mode solution for personalized thermal management aimed at seasonal temperature fluctuations [2]. Pasupathi et al. (2020) applied hybrid nano/paraffin phase change materials in solar thermal systems, demonstrating enhanced thermal performance and energy capacity [3]. Ansu et al. (2021) improved the thermal energy storage behavior of polyethylene-glycol-based phase change composites and aluminum oxide nanoparticles for solar thermal applications, aiming to enhance solar thermal conversion efficiency and thermal conductivity [4]. Zheng et al. (2017) explored the use of microencapsulated phase change materials in solar thermal conversion systems to understand heating efficiency and system reliability [5]. Tyagi et al. (2021) discussed the role of thermal energy storage (TES) in measuring the energy performance of buildings, integrating a list of phase change materials for energy-efficient buildings along with their thermal properties [6]. Li et al. (2020) presented a dual-mode device integrating daytime radiative cooling and solar heating, achieving year-round energy savings in buildings through engineered surface morphology and optical properties [7]. In addition, other researchers have studied solar heating equipment and systems. Hassan et al. (2020) conducted experimental research on the performance of a novel solar air heater (SAH) and a tubular solar air heater (TSAH). The results indicate that compared to the flat-plate solar air heater (FSAH), TSAH exhibits higher efficiency, output power, and outlet air temperature, as well as lower top heat losses [8]. Vengadesan et al. (2020) presented the latest developments, practical techniques, economic significance, requirements, and obstacles of solar water heaters, along with the application of solar energy for water heating [9]. Munusamy et al. (2023) investigated the performance of a parabolic trough solar water heater employing copper concave tubes with aluminum-coated pipe slots [10]. Khimsuriya et al. (2022) stated that solar air heaters are the most promising devices for providing adequate heating of working fluids at the lowest possible heating process cost [11]. Kumar et al. (2021) proposed an innovative hybrid system with dual objectives of simultaneously heating air and water. To enhance thermal performance, the inner surface of rectangular aluminum tubes in the air heater and the copper absorber plate in the water heater underwent roughening treatment using a pressure blasting technique. Additionally, the convective heat transfer performance was enhanced using solar glycol (SG) nanofluid based on multi-walled carbon nanotubes (MWCNTs) [12]. Mayer et al. (2020) investigated the lifecycle environmental impacts in the optimization of small-scale hybrid renewable energy systems, aiming to fill this gap by providing a multi-objective design framework for household-scale systems based on technical modeling of several typical components [13].

Some researchers have focused on theoretical aspects. Zhang et al. (2020) explored a photocatalytic phase-change mechanism for collective solar and thermal energy harvesting, enabling storage and release of energy for high-temperature thermal applications [14]. Abokersh et al. (2021) emphasized the sustainability of emerging solar district heating technologies for the promotion of the concept of near-zero-energy buildings [15]. Furthermore, Dehghan et al. (2021) reviewed the technical and economic feasibility of solar thermal water systems in the Middle East region, highlighting the benefits and challenges of integrating solar thermal technologies into the region's energy landscape [16]. Koçak et al. (2020) reviewed the latest trends in sensible thermal energy storage systems and materials used in solar industrial applications, focusing particularly on sustainability. Their aim was to provide information for further research and development, making solar heating a cost-effective method to meet the growing energy demands of the industrial sector [17]. Abokersh et al. (2021) evaluated the technical and economic benefits of various control strategies for heat pumps integrated into solar-assisted district heating systems (SDHS) [18]. Hosseini et al. (2022) proposed a novel robust model predictive control (MPC) method for online energy scheduling in multiple commercial buildings, including standalone HVAC systems, ESS, and uncontrollable loads. Their method aims to minimize the expected total

energy cost while ensuring thermal comfort for occupants in the presence of uncertainty in electricity market pricing [19]. Arteconi et al. (2017) presented existing configurations of thermal energy storage (TES) systems coupled with heat pumps in industrial buildings and developed a dynamic simulation model to represent their behavior. It was found that employing TES leads to an increase in energy demand, but costs can be reduced when there is a considerable difference in electricity prices between peak and off-peak periods [20]. Seeking efficient thermal energy storage solutions, Li et al. (2020) proposed an IoT-based tuning approach to enhance energy efficiency of solar water heating systems [21]. Kalbasi et al. (2021) focused on finding optimal residential-scale solar heating stations in Belgium, considering all system losses and conducting economic analyses [22]. Additionally, some researchers have investigated the installation angle and area of solar panels. Han et al. (2024) studied the usage of solar heating in traditional buildings in western China and investigated the optimal installation angles and areas for solar panels [23]. Siraki et al. (2012) proposed a simple method based on an improved sky model for calculating the optimal installation angle for urban applications [24]. Sharma et al. (2020) proposed a method to maximize the annual output of photovoltaic (PV) panels by determining the optimal tilt angle [25]. Schuster et al. (2020) proposed a technique involving using actual historical solar spectra to rigorously evaluate the tilt of panels at specific locations [26]. Zhong et al. (2020) introduced a novel spatial optimization problem, namely the Maximum Photovoltaic Panel Coverage Problem (MPPCP), for the layout design of solar photovoltaic panels [27]. Gardashov et al. (2020) proposed a novel method for determining the optimal orientation of each solar panel. This method is based on a simple solar radiation mathematical model that identifies the solar energy at any given time and location, while also accounting for solar shading caused by the surrounding topography. Identifying the optimal orientation for solar panels in mountainous regions is particularly beneficial [28]. In the field of solar heating technology, Meng et al. (2019) provided a comprehensive overview of its research status and development trends. They discussed advancements in solar heat collection and heating implementation, emphasizing the need for improved collection technologies and thermodynamic analysis [29]. Furthermore, Khimsuriya et al. (2022) conducted a comprehensive review of artificially roughened solar air heating technology, contributing to a better understanding and optimization of solar heating systems [11]. From the literature, it is evident that research in solar heating technology is advancing, with a focus on improving energy efficiency, thermal storage, and system reliability. Collaborative efforts between researchers and industry professionals are crucial for further developing and implementing solar heating systems to seek sustainable energy solutions.

For both domestic and foreign Tibetan researchers, the study of Thangka has always been a hot topic. Researchers have already investigated the similarities and differences between Thangka carvings and embroidered images based on highlights, shadows and edge information. They proposed three new features: Consistency of Illumination Direction (CID), Distribution of Highlights and Shadows along Edges (DHSE), and Edge Similarity in Different Channels (ESDC). The distribution of Thangka image samples in these feature spaces has also been analyzed [30]. Additionally, it was proposed to explore the protection and inheritance of traditional Thangka techniques through virtual reality technology and expanding the dissemination of Thangka through the power of the internet [31]. However, research related to Thangka preservation is still in its early stages, with relatively more studies conducted abroad and preceding those in domestic research. With the increasing attention to Thangka preservation domestically, research on Thangka protection has become increasingly important. Some researchers have conducted inspections of the landscapes surrounding Thangka images, revealing insights crucial for the development of cultural industries and heritage conservation. Through bibliometric analysis, researchers have depicted the current status of Thangka image studies, providing valuable information for stakeholders involved in Thangka preservation efforts [32]. Researchers have conducted a series of studies on Thangka diseases. Zhu et al. analyzed the physicochemical factors contributing to Thangka damage, such as temperature, humidity, light exposure, and air

quality, and pointed out the impact of the internal environment in which Thangka are stored on Thangka preservation, advocating for enhanced protective measures [33]. Some researchers have investigated Thangka cleaning methods, summarizing dry cleaning and wet cleaning methods [34]. Additionally, some scholars have utilized computer image processing techniques to simulate the restoration of Thangka images, providing new approaches for Thangka preservation [35]. A notable study has delved into the use of virtual reality (VR) technology to preserve traditional Thangka techniques. By embracing virtual reality, this research has opened up new avenues for the preservation and dissemination of Thangka practices [31].

While numerous researchers have studied solar heating, few have integrated solar energy systems with the preservation of Thangka art. This study focuses on the nearly zero-energy design of Thangka exhibition halls. By harnessing abundant local solar energy resources and installing solar panels on rooftops, heating sources are provided for both the exhibition halls and storage rooms, ensuring compliance with the temperature requirements for Thangka preservation and ensuring human thermal comfort. Additionally, by studying the optimal installation angles and areas of solar panels in the region, along with the thermal-economic feasibility of meeting indoor temperature requirements, renewable energy optimization strategies for Thangka exhibition halls' protection and renovation have been proposed. The integration of traditional heritage conservation with modern technology enhances the adaptability and sustainability of architectural spaces.

2. Materials and Methods

2.1. Research Process

This study was conducted along two main directions, as illustrated in Figure 1, namely, preliminary preparation and the setup of the solar panel system. The preliminary preparation included utilizing BESI simulation in Sware software (2023) to obtain the hourly temperature data for the Malkang area throughout the year, exporting hourly solar radiation data using DeST software (2020) as a reference, setting photovoltaic conversion efficiency and solar radiation intensity variables using Python (3.10), simulating the effective utilization rate of solar panels, and determining the optimal temperature range for preserving Thangka (16–19 degrees Celsius) and optimal temperature range for human thermal comfort during different time periods. The setup of the solar panel system involves calculating the optimal azimuth angle and tilt angle of the solar panels, as well as determining the optimal layout area of the solar panels. Following the establishment of the optimal temperature range for preserving Thangka, temperature studies were conducted separately for the exhibition hall and the storage room. The research on calculating the optimal azimuth angle and tilt angle of the solar panels employed the method of controlling variables to identify the approximate range of optimal tilt angles and azimuth angles. Subsequently, the annual variation pattern of solar energy capture with respect to the tilt angle and azimuth angle in the Malkang area of Sichuan province was determined through optimization solving. Finally, the optimal azimuth angle and tilt angle were obtained through optimization solving. The study on calculating the optimal layout area of the solar panels involved analyzing and calculating the temperature increases required for the exhibition hall and the storage room and then calculating the heating energy consumption during the peak heating months for both areas based on the building's heating energy requirements. The areas of solar panels required to achieve near-zero energy consumption for heating in the exhibition hall and the storage room, as well as the areas of solar panels required to raise the temperature for Thangka preservation, were then calculated, and their respective proportions were determined to derive the optimal layout scheme for solar panel areas.

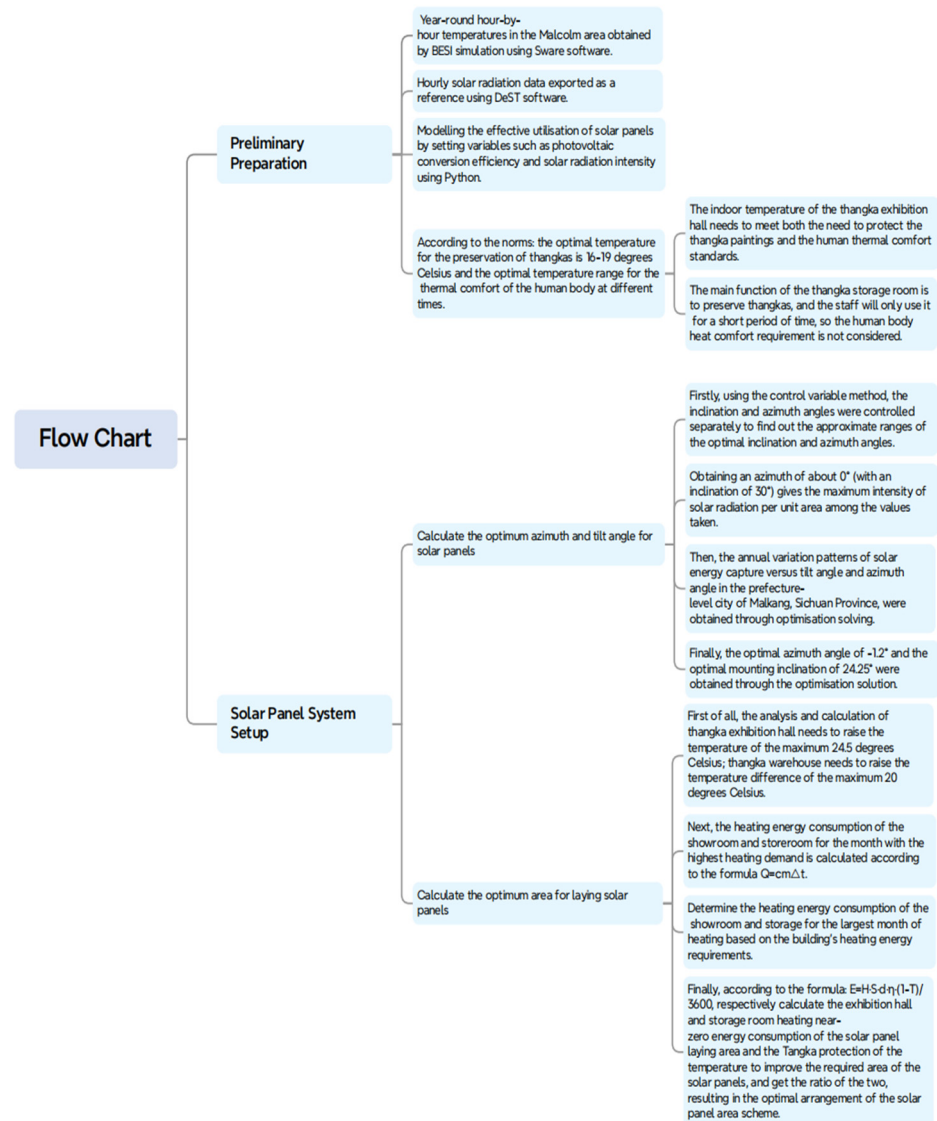


Figure 1. Flow chart of the study.

2.2. Solar Heating Mechanism

The research principle of this study involves several steps. Firstly, the energy consumption of the Thangka exhibition hall was predicted using Sware software. Then, the local meteorological parameters in the Malkang area were integrated using DeST software to derive the local solar conditions. Subsequently, parameterized active heating design was employed, with a solar panel set above the exhibition hall at an appropriate angle and sufficient area. Python was utilized to set variables such as photovoltaic conversion efficiency and solar radiation intensity to simulate the effective utilization rate of the solar panels. Combining Sware software, solar energy was converted into the heating energy required by the building. Optimal parameters such as the optimal area, angle, and economic benefits of the photovoltaic panels were determined. Finally, an optimization solution satisfying the protection requirements of the Thangka exhibition hall was obtained using formulas, as depicted in Figure 2.

The principle of using solar energy for passive and active coupling heating to improve the temperature in the Thangka exhibition hall is based on the integration of rooftop solar panels, which efficiently capture solar radiation and complement the urban power grid to provide dual power sources for the heating system equipment. This system, combined with the insulation effect of the building’s own materials and maintenance structure, forms

the heating system of the Thangka exhibition hall, ultimately meeting the requirements for Thangka protection and human thermal comfort (Figure 3).

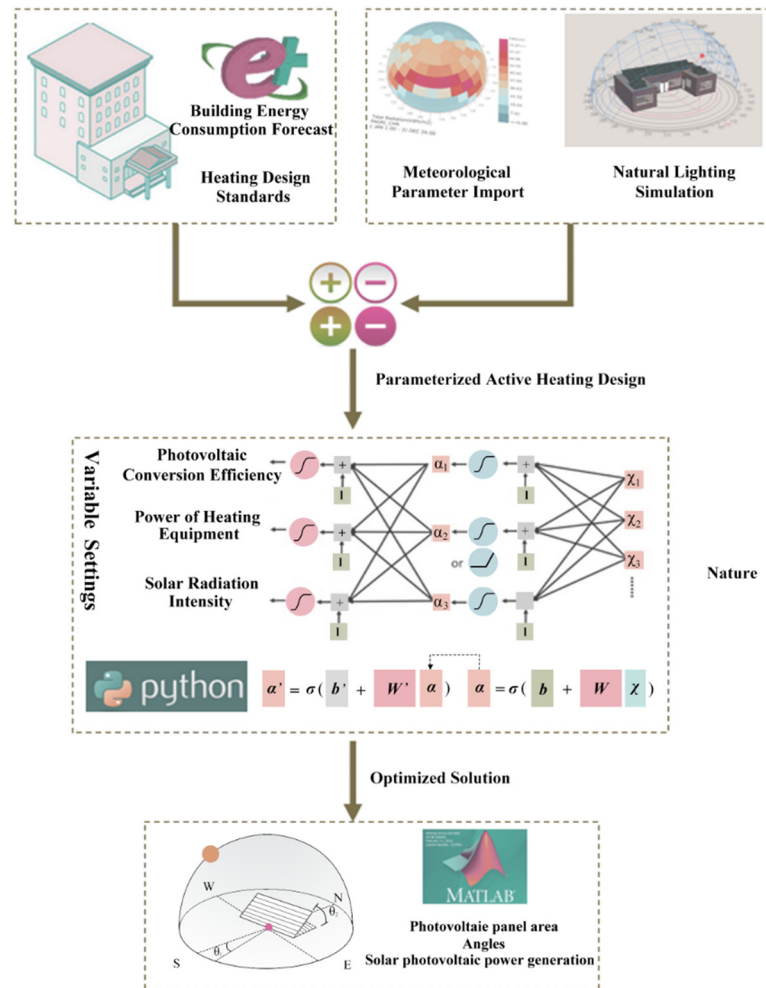


Figure 2. Solar energy system operation mechanism.

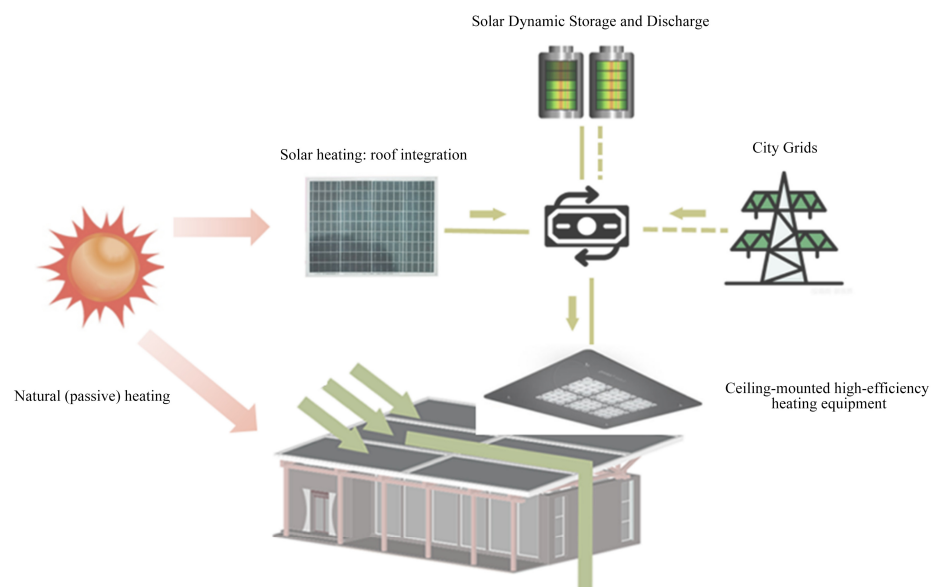


Figure 3. Active and passive solar energy model.

2.3. Thangka Exhibition Room Parameter Setting

This study is based on relevant research on Thangka preservation. The architectural model of the exhibition hall was designed and constructed using AutoCAD (2021) software. Subsequently, the model was imported into SU and BES1 (Building Energy Simulation, 2023) for solar radiation simulation and energy consumption simulation. The simulation work was conducted in Zhibo Village, Malkang City, Aba Tibetan and Qiang Autonomous Prefecture, Sichuan Province, China, with local meteorological parameters incorporated into the software. The main purpose of the simulation was to calculate the energy consumption generated by the Thangka exhibition hall during operation under different temperature conditions from both active and passive perspectives, and to supplement its energy consumption using solar energy systems to achieve near-zero energy consumption. Building model accuracy is crucial in the simulation process, so we made corresponding parameter settings for the exhibition hall, storage room, building height, orientation, heating time, roof tilt angle, and door and window opening methods to ensure the integrity of the building model. The architectural parameter structure is shown in (Figure 4). Specific parameters are shown in Table 1.

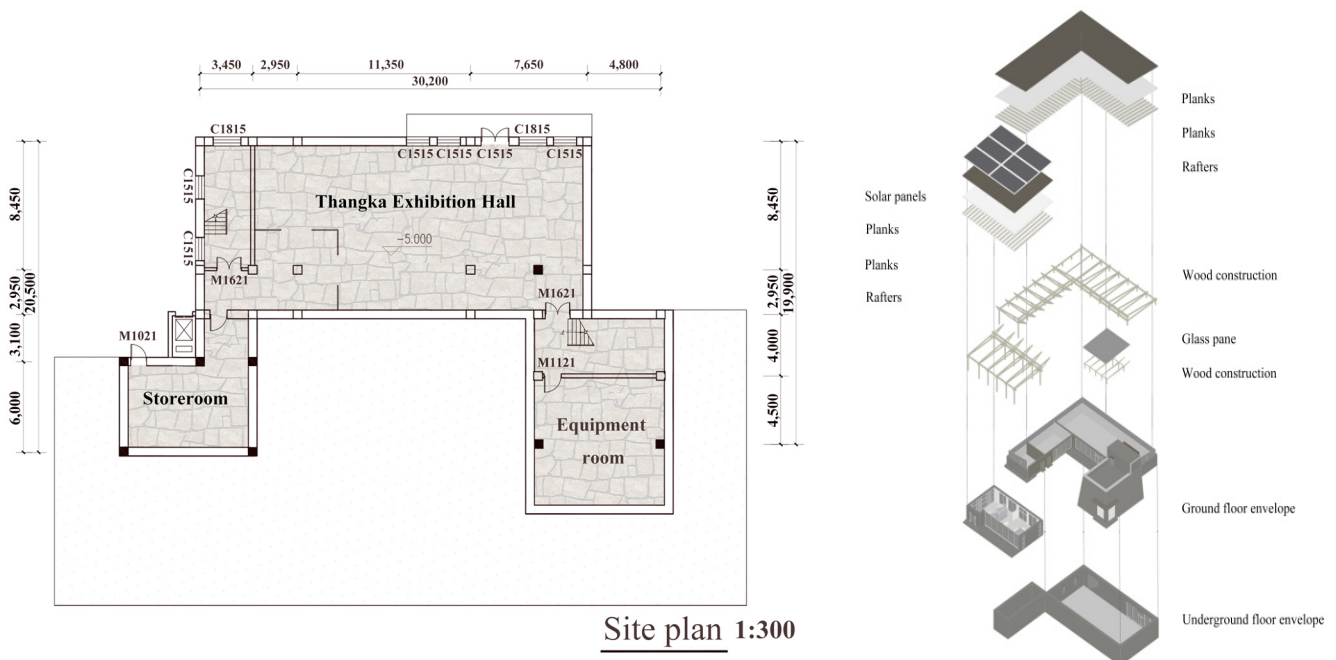


Figure 4. Building model setting.

Table 1. Building model parameterization.

Category	Detail
Exhibition hall area	240.648 square meters
Storage room area	43.4 square meters
Building height	5.2m
Building orientation	East–west orientation
Heating period	24 months
Angle of dip of roof	20°
Door and window opening method	Half-open

Throughout the entire building simulation process, we focused on using the BES1 tool to simulate the heating energy consumption of the Thangka exhibition hall. To ensure more accurate results, we refined the relevant parameters of the building model. Since

the structural materials and properties of the materials have a significant impact on the simulation results, we also set the building materials and their corresponding properties in the software. This was to meet the indoor temperature requirements of the Thangka exhibition hall from a passive insulation perspective and integrate the building materials with the local architectural environment seamlessly, avoiding any abruptness. The detailed parameters of the building's structural materials and their properties are listed in Table 2.

Table 2. Building structural materials and nature of materials.

(a) Building structural materials						
Architectural Parts	Structural Measures					
Wall construction	Cement mortar, lime mortar, reinforced concrete, extruded polystyrene foam (with skin)					
Flooring	Cement mortar, reinforced concrete					
Roofing	Cement mortar, lime mortar, reinforced concrete, gravel, concrete with pebbles ($\rho = 2300$), extruded polystyrene foam (with skin), aerated concrete, foam concrete ($\rho = 700$).					
Doors	Single-layer solid wood					
Windows	12A steel–aluminum single-frame double glazing window (average).					
(b) Nature of materials						
Material Name	Thermal Conductivity Coefficient λ	Heat Storage Coefficient S	Density ρ	Specific Heat Capacity C_p	Vapor Permeability Coefficient μ	Solar Heat gain Coefficient
	W/(m·K)	W/(m ² ·K)	kg/m ³	J/(kg·K)	g/(m·h·kPa)	
Cement mortar	0.930	11.370	1800.0	1050.0	0.0210	
Lime mortar	0.810	10.070	1600.0	1050.0	0.0443	
Steel-reinforced concrete	1.740	17.200	2500.0	920.0	0.0158	
Gravel stone and pebble concrete ($\rho = 2300$)	1.510	15.360	2300.0	920.0	0.0173	
Extruded polystyrene foam plastic (with skin)	0.030	0.340	35.0	1380.0	0.0000	
Aerated concrete, foam concrete ($\rho = 700$)	0.180	3.100	700.0	1050.0	0.0998	
Porous concrete brick (190 six-hole brick)	0.750	7.490	1450.0	709.4	0.0000	
12A steel–aluminum single-frame double-glazed window (average)		3.900				0.652
Wooden		4.700				0.566

According to the “Code for Museum Building Design” (JGJ66-2015) 10.3.2 [36], in severely cold regions, the indoor design temperature of museum exhibition halls' main display areas and working areas should be maintained at between 18 and 24 degrees Celsius. According to the “Code for Thermal Design of Civil Buildings” (GB 50176-2016) [37], the region of Maerkang belongs to the cold climate zone among the five climate zones in China. Therefore, the indoor temperature of the Thangka exhibition hall should meet the standard requirements, namely, to be maintained within the range of 18–24 °C. Additionally, based on the average temperatures from May to July in the Tibet Museum, set at 16 to 19 °C [38], we believe this temperature range is relatively balanced and is the optimal temperature for Thangka preservation.

According to Formula (1), a relationship between energy and temperature can be established, representing the energy requirement for each one-degree Celsius increase in indoor temperature. In the formula, Q represents the generated energy in joules (J); C denotes the specific heat capacity of air in joules per kilogram per degree Celsius (J/(kg·°C)); and ΔT indicates the numerical value of the temperature change produced, measured in degrees Celsius (°C).

$$Q = CM\Delta T \quad (1)$$

2.4. Solar Energy System Setup

- 1 Installation of solar panels: Due to the ample sunlight conditions in the Malkang area, solar resources are readily available, making it feasible to utilize solar energy in this study. Additionally, as the Thangka exhibition hall is situated below the intangible cultural heritage exhibition hall, to primarily meet the building's functional requirements, we have positioned the solar panels on the roof of the intangible cultural heritage exhibition hall (highlighted in orange in Figure 5). The relevant

heating equipment is arranged inside the intangible cultural heritage exhibition hall (highlighted in red in Figure 5). Heat pipes are embedded in the walls and extend beneath the floor of the Thangka exhibition hall (highlighted in green in Figure 5), allowing for indoor heating from both the walls and the floor, ensuring that the indoor temperature reaches the required level for preserving Thangka and providing human thermal comfort.

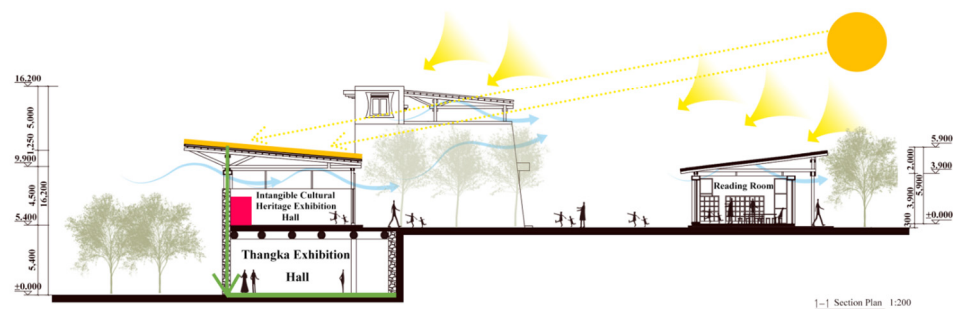


Figure 5. Solar energy panel layout status.

- 2 Optimal mounting angle for solar panels: In this study, we used hourly solar radiation data from the DeST software (h) as a reference. The optimal installation angle of the solar panels was calculated using Formulas (2)–(5) [23], where H_T is the total radiation in W/m^2 ; H_{bT} is the direct radiation in W/m^2 ; H_{dT} is the diffuse sky radiation in W/m^2 ; H_{rT} is the ground-reflected radiation in W/m^2 ; H_{DN} is the normal radiation intensity in W/m^2 ; ε is the tilt angle of the solar panel collector; β is the solar azimuth angle; α is the solar altitude angle; A is the orientation angle of the solar panel collector; H_d is the diffuse sky radiation intensity in W/m^2 ; ρ is the ground reflection coefficient; and H is the horizontal total radiation intensity in W/m^2 . The selected analysis location is Zhibo Village, Songgang Town, Malkang City, Aba Prefecture, Sichuan Province, China, with coordinates at longitude 102.104722 and latitude 31.91474. The selected range of azimuth angles includes -65 to 65 , covering directions from east to west. Regarding tilt angles, values from 0 to 90 (representing horizontal to vertical directions) were considered. Using Excel (2016) planning and solving, by exploring different combinations of tilt angles and azimuth angles, we determined the pattern of solar capture in response to changes in installation angles. The angle with a relative loss of 0.0% was determined as the optimal installation tilt angle, along with the optimal azimuth angle. This analysis aims to alleviate the impact of solar panel angles on installation area requirements and thermal economics.

$$H_T = H_{bT} + H_{dT} + H_{rT} \quad (2)$$

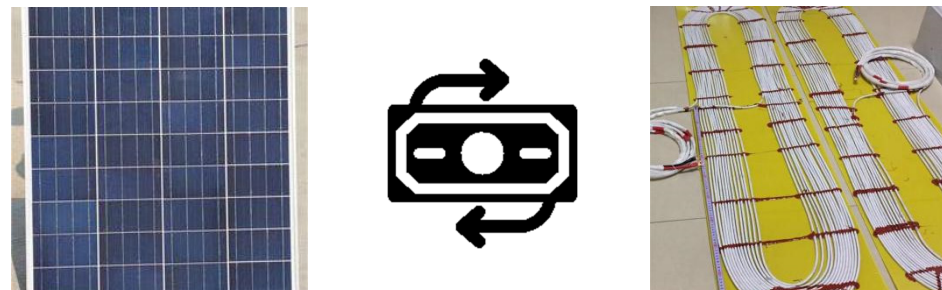
$$H_{bT} = H_{DN} \cdot (\cos \varepsilon \cdot \sin \beta + \sin \varepsilon \cdot \cos(A - \alpha)) \quad (3)$$

$$H_{dT} = H_d \cdot (1 + \cos \varepsilon) / 2 \quad (4)$$

$$H_{rT} = \rho \cdot H \cdot (1 - \cos^2 \varepsilon) / 2 \quad (5)$$

- 3 Conversion and loss rates of solar panels: This study employs a novel ceramic-aluminum composite solar panel, which is primarily composed of aluminum alloy substrate, flow-collecting pipes, and a nanostructured absorptive coating. The main materials used in its development include black ceramic powder and a corrosion-resistant aluminum alloy. This solar panel exhibits an exceptional thermal conductivity efficiency of 0.98, a collector efficiency of 43.6%, and a sunlight absorption rate of 0.96% on its surface. The conversion efficiency is shown schematically in Figure 6. With its high conversion rate and low loss rate, this solar panel is exceptionally well suited for use in heritage buildings [39].

A collector efficiency of 43.6%



Thermal conductivity efficiency:0.98

Figure 6. Solar panel conversion efficiency.

- 4 The optimal laying area for solar panels: Formula (6) represents the daily average solar radiation in KJ/m^2 for the month with the highest heating demand. Formula (7) is used to calculate the heating energy consumption of the solar panels. In this formula, “ E ” represents the energy generated by the solar panels; “ H ” represents the average daily solar radiation in KJ/m^2 ; “ H_0 ” indicates the monthly average solar radiation; “ S ” represents the area covered by the solar panels, measured in square meters (m^2); “ d ” represents the number of days the solar panels operate, measured in days; “ η ” represents the conversion efficiency of the solar panels, expressed as a percentage (%); and “ T ” represents the conversion loss rate of the solar panels, also expressed as a percentage (%).

$$H = H_0 / 30 \quad (6)$$

$$E = H \cdot S \cdot d \cdot \eta \cdot (1 - T) / 3600 \quad (7)$$

3. Current Situation and Requirements for Thangka Conservation

The materials used to make Thangka are all organic fiber products, including silk, wool, hemp, cotton, and other textile products, all of which come from natural biopolymers in the environment and possess a cellular-like structure and moisture absorption capability. Therefore, Thangka is very susceptible to temperature changes. When the temperature is too high and lasts for a long time, Thangka will shrink, crack, and deform. Similarly, high temperature and humidity lead to the synthesis of hydrogen peroxide from active oxygen and water vapor in the atmosphere, accelerating the decomposition of cellulose and damaging silk textiles [33]. Moreover, elevated temperatures are highly conducive to the growth of mold, promoting the proliferation of fungi, pests, and microorganisms, leading to the aging of Thangka materials. When temperatures decrease, Thangka becomes

prone to brittleness, warping, color cracking, and reduced mechanical strength, and when the temperature drops below 0 degrees Celsius, moisture inside the materials may freeze, causing structural changes and damage to the Thangka [40]. Currently, the protection environment for Thangka largely fails to meet the temperature requirements necessary for their preservation. Thangka displayed in exhibition halls are often directly hung on walls, exposed to the air. Consequently, temperature is the most crucial consideration in the design of Thangka exhibition halls. Throughout the operating cycle of the exhibition hall, temperature fluctuations must be controlled to a minimum level and meet the temperature requirements for Thangka preservation. Figure 7 depicts some of the damage caused to Thangka due to improper preservation methods.

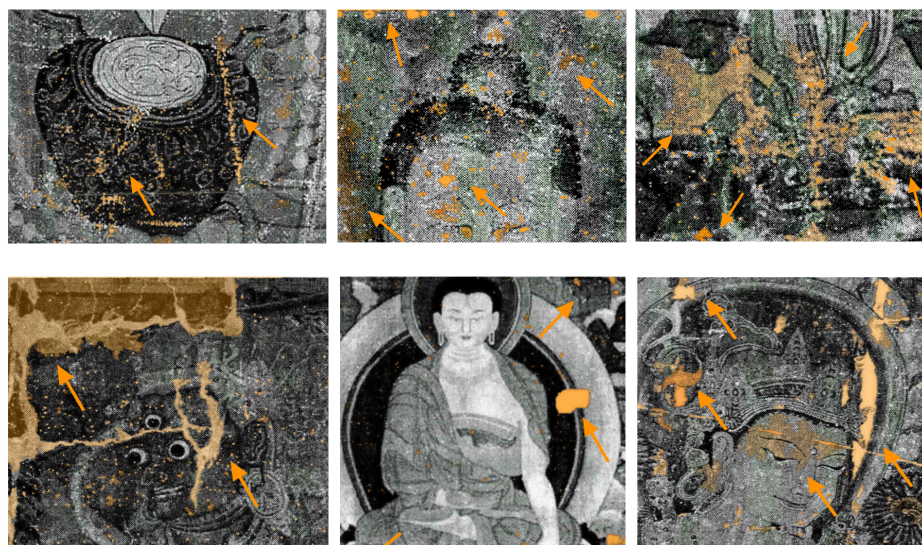


Figure 7. Thangka protection status.

4. Local Climate Conditions

1. Geographical position:

The case study building is located in Zhibo Village, Songgang Town, Malkang City, Aba Tibetan and Qiang Autonomous Prefecture, Sichuan Province, China. It is situated on the southern edge of the Qinghai–Tibet Plateau, in the northwest part of the Sichuan Basin, with Aba and Hongyuan Grasslands to the north, and adjacent to the Wolong Giant Panda Nature Reserve and Xiaojin Siguniang Mountain to the south. It is 365 km away from the provincial capital Chengdu, covering an area of 6633 square kilometers. The city center is located at 102°13' east longitude and 31°55' north latitude. Songgang Town is located 15 km west of Malkang City, with an average altitude of 2540 m above sea level, and covers a total area of 224 square kilometers. Zhibo Village is situated in the southeast of Songgang Town, 1.5 km from the town government seat. It borders Ha Piao Village to the east, Songgang Village to the west, Jiao Muzu Village to the south, and Pu'erma Village to the north, with a total area of 30 square kilometers (Figure 8).

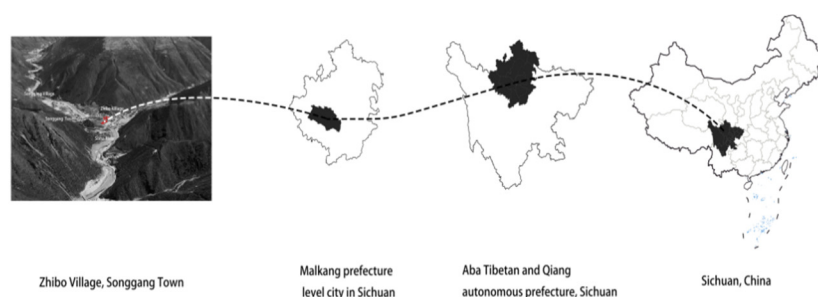


Figure 8. Geographic information map of Malkang.

2. Temperature:

The warm season lasts for 4.2 months, from May 11 to September 17, with an average daily high temperature above 63 °F. The hottest month of the year in Aba is July, with an average high of 68 °F and low of 45 °F. The cold season lasts for 3.0 months, from November 24 to February 25, with an average daily high temperature below 43 °F. The coldest month of the year in Aba is January, with an average low of 10 °F and high of 37 °F (Figure 9).

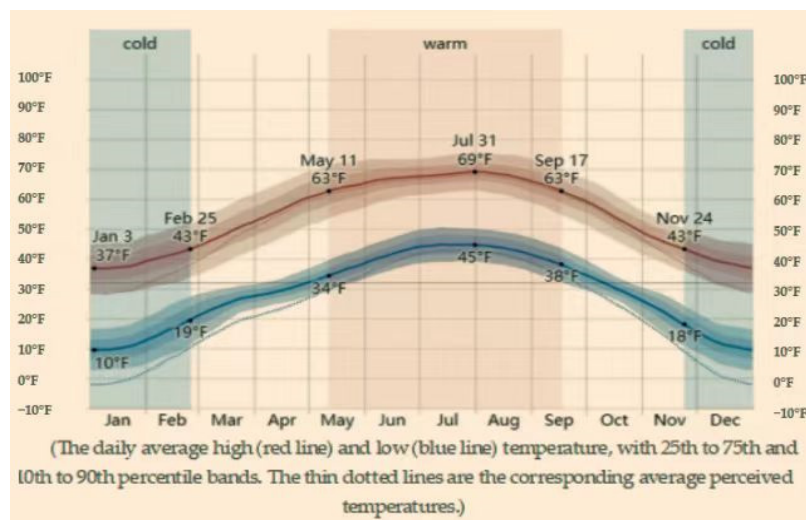


Figure 9. The Malkang temperature conditions.

3. Solar Energy:

This section discusses the total daily incident shortwave solar energy reaching the surface of the ground over a wide area, taking full account of seasonal variations in the length of the day, the elevation of the Sun above the horizon, and absorption by clouds and other atmospheric constituents. Shortwave radiation includes visible light and ultraviolet radiation. The average daily incident shortwave solar energy experiences significant seasonal variation over the course of the year. The brighter period of the year lasts for 4.3 months, from April 13 to August 23, with an average daily incident shortwave energy per square meter above 6.4 kWh. The brightest month of the year in Aba is May, with an average of 7.1 kWh. The darker period of the year lasts for 3.1 months, from November 4 to February 6, with an average daily incident shortwave energy per square meter below 4.3 kWh. The darkest month of the year in Aba is December, with an average of 3.6 kWh (Figure 10).

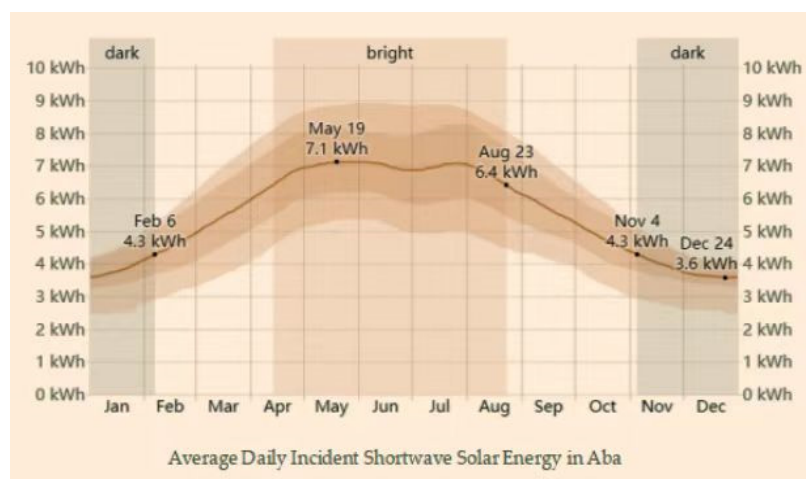


Figure 10. The Malkang solar energy situation.

5. Results and Discussion

5.1. Indoor Temperature Optimization

This study involves the simulation and analysis of the indoor thermal environment and thermal comfort of various functional rooms within a building, as shown in the diagram. It is observed that the fluctuations in indoor temperature are positively correlated with outdoor temperature fluctuations. Furthermore, the indoor temperature remains relatively stable at the minimum comfort temperature during the period from July to August. However, for the rest of the year, the indoor temperature falls short of meeting the basic requirements for thermal comfort. By calculating the temperature difference between indoor temperature and the minimum comfort temperature, the required temperature adjustments are determined. These adjustments are made considering the diverse functional requirements of different rooms within the building.

Of particular significance is the Thangka Exhibition Hall, which not only serves tourists but also requires an indoor temperature that meets human thermal comfort standards. This ensures that visitors can comfortably enjoy the Thangka exhibits for extended periods. Additionally, to preserve the Thangka for long-term viewing, environmental monitoring is necessary to maintain appropriate and consistent temperature and humidity levels. Since the backing fabric of the Thangka is cotton, exposure to fluctuating temperature and humidity can lead to fiber aging, chemical bond breakage, loss of fiber elasticity and toughness, and uneven fabric shrinkage, all of which can seriously damage the appearance of the Thangka.

The simulation results, as shown in Figure 11, divide the year into four phases to simultaneously meet human thermal comfort and Thangka preservation temperature requirements:

1. From October to April each year, the lowest indoor temperature occurs on December 11th, reaching -7°C . The range for the minimum and maximum comfortable temperatures is between 17.5°C and 24.5°C . To meet the Thangka preservation requirements, the temperature needs to be maintained at $16\text{--}19^{\circ}\text{C}$.
2. In May and September each year, the average indoor temperature is 14°C , with the minimum and maximum values of thermal comfort temperature being 18°C and 25°C , respectively. To meet the Thangka preservation requirements, the temperature needs to be maintained at $16\text{--}19^{\circ}\text{C}$.
3. In June and August each year, the average indoor temperature is 16°C , with the minimum and maximum values of thermal comfort temperature being 18.5°C and 25.5°C , respectively. To meet the Thangka preservation requirements, the temperature needs to be maintained at $16\text{--}19^{\circ}\text{C}$.
4. In July each year, the average indoor temperature is 17.5°C , with the minimum and maximum values of thermal comfort temperature being 19°C and 26°C , respectively. To meet the Thangka preservation requirements, the temperature needs to be maintained at $16\text{--}19^{\circ}\text{C}$.

In conclusion, we have compiled the required increases in indoor temperature as follows:

1. From October to April each year, the indoor temperature should be maintained between 17.5°C and 19°C . However, considering the lowest temperature recorded on December 11th, an increase of at least 24.5°C is required to meet the requirements for protecting the Thangka.
2. In May and September each year, the indoor temperature should be controlled at $18\text{--}19^{\circ}\text{C}$, requiring an increase of $4\text{--}5^{\circ}\text{C}$.
3. In June and August each year, the indoor temperature should be controlled at $18.5\text{--}19^{\circ}\text{C}$, requiring an increase of $2.5\text{--}3^{\circ}\text{C}$.
4. In July each year, since the minimum temperature for human thermal comfort is equal to the optimal temperature range for Thangka preservation, the indoor temperature should be controlled at 19°C , requiring an increase of 2.5°C .

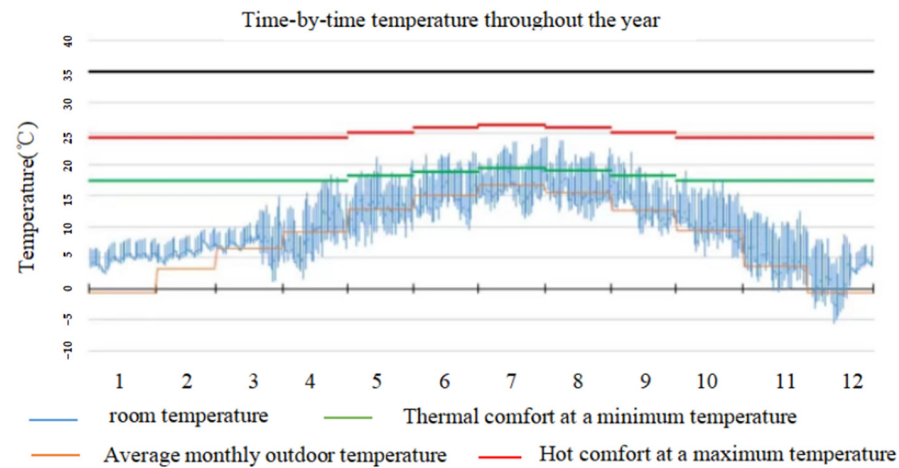


Figure 11. Hourly temperature variations throughout the year in the Thangka exhibition hall.

Based on the temperature simulation results from the storage room, as shown in Figure 12, it can be observed that the overall temperature fluctuations are similar to those of the exhibition hall. However, the temperature variations throughout the day are relatively small. Considering that the main function of the storage room is to preserve the Thangka and it is only briefly used by staff, the requirement for human thermal comfort was not taken into account. The primary concern for the room is to meet the temperature requirements for preserving the Thangka. Specifically, it is only necessary to ensure that the indoor temperature remains within the range of 16–19 degrees Celsius. We have also divided it into four time periods and summarized the temperature increases needed indoors as follows:

1. From October to April each year, the minimum indoor temperature was $-4\text{ }^{\circ}\text{C}$, and it should be maintained within the range of $16\text{--}19\text{ }^{\circ}\text{C}$. An increase of at least $20\text{ }^{\circ}\text{C}$ required to meet the temperature requirements for preserving Thangka.
2. In May and September each year, with an average indoor temperature of $13\text{ }^{\circ}\text{C}$, the indoor temperature should be controlled within the range of $16\text{--}19\text{ }^{\circ}\text{C}$. Currently, an increase of $3\text{--}6\text{ }^{\circ}\text{C}$ is needed.
3. In June and August each year, with an average indoor temperature of $15\text{ }^{\circ}\text{C}$, the indoor temperature should be controlled within $16\text{--}19\text{ }^{\circ}\text{C}$. Currently, an increase of $1\text{--}4\text{ }^{\circ}\text{C}$ is required.
4. In July each year, with an average indoor temperature of $17\text{ }^{\circ}\text{C}$, the indoor temperature should be controlled within $16\text{--}19\text{ }^{\circ}\text{C}$. Currently, an increase of $0\text{--}2\text{ }^{\circ}\text{C}$ is needed.

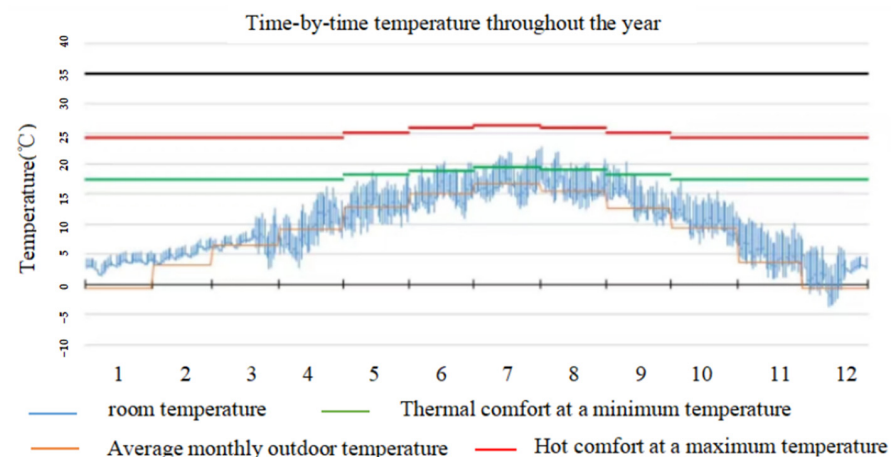


Figure 12. Hourly temperature variations throughout the year in the Thangka exhibition hall storage room.

5.2. Solar Panel Optimization Mode

1 Optimal installation angle of solar panels:

Based on Figure 13, we were able to find that a solar panel at an azimuth angle of 0° , regardless of the value of the solar panel mounting tilt angle, will reach the maximum value under its own tilt angle. At an azimuth angle of 0° and a mounting tilt angle of 30° , the intensity of solar radiation per unit area reaches the maximum value. In order to verify that the optimal value of the mounting azimuth angle is 0° , we kept the tilt angle unchanged, and changed the azimuth angle to -15° , 0° , and 15° , as shown in Figure 14. It was found that the intensity of solar radiation per unit area is at its maximum at 0° and reaches the maximum value when the inclination angle is 30° . So, the optimal installation tilt angle is approximately 30° , and the optimal azimuth angle is approximately 0. To further elucidate the optimal tilt angle and azimuth angle of the solar panels based on this, we obtained the optimal values for the tilt angle and azimuth angle in Malkang Prefecture of Sichuan Province through optimization calculations, as shown in Figure 15. Through optimization, the optimal azimuth angle was determined to be -1.2° , and the optimal installation tilt angle was 24.25° . With this installation tilt angle and azimuth angle, the entire solar panel can receive the maximum solar radiation, maximizing the efficiency of solar energy capture.

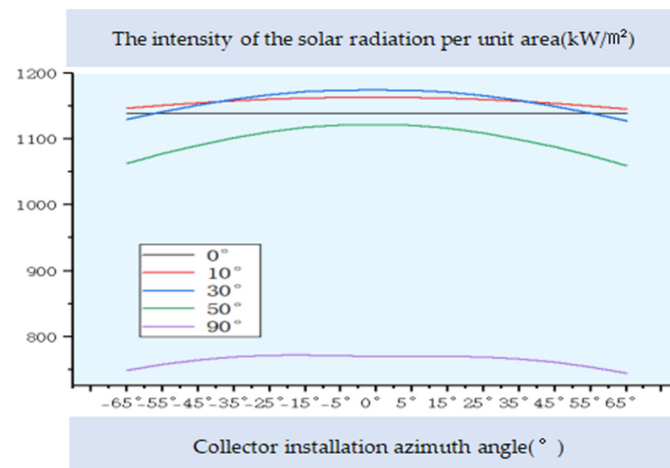


Figure 13. Effect of different azimuth angles on solar radiation capture under several inclination conditions in Malkang.

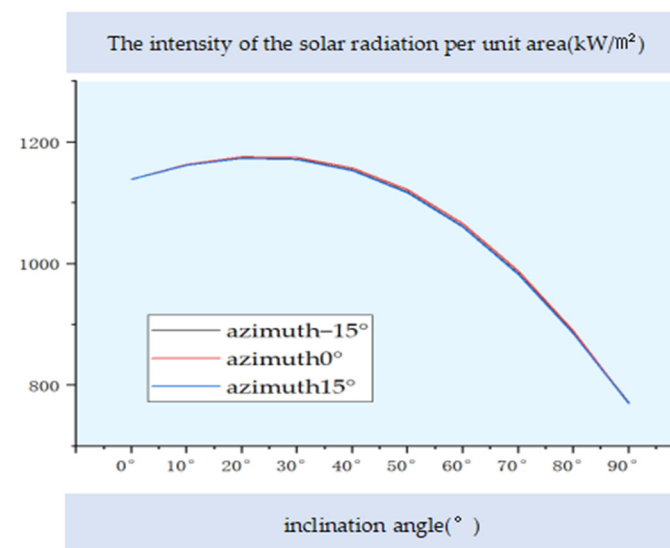


Figure 14. The influence of different inclination angles on the solar radiation capture under several azimuth conditions in Malkang.

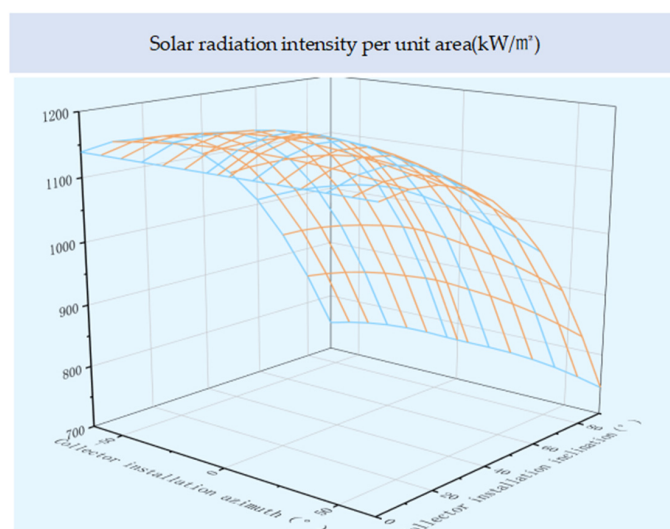


Figure 15. The annual law of solar energy capture capacity in Malkang changes with inclination angle and azimuth angle.

2 Minimum installation area of the solar panels:

To reduce the impact of solar panel coverage on the building and ensure that the temperatures in both the Thangka exhibition hall and storage room meet the requirements, we need to determine the minimum area for solar panel installation based on the incremental indoor temperature. Firstly, we must establish the required temperature increment indoors. Secondly, we need to investigate how much electrical energy the solar heating equipment needs to provide to ensure that the indoor temperature reaches the desired value. Then, we need to determine the photothermal conversion efficiency of the solar system to achieve the target area of the solar panel through a temperature increase. According to the temperature analysis results for the Thangka exhibition hall, it is necessary to increase the temperature by at least $24.5\text{ }^{\circ}\text{C}$ to meet the temperature requirements and ensure human thermal comfort. According to Table 1, we know that the volume of the exhibition hall is 1251.3696 m^3 and the volume of the storage room is 225.68 m^3 , with an air density of 1.29 kg/m^3 and an air specific heat capacity of $1000\text{ J/(kg}\cdot^{\circ}\text{C)}$. Through the calculation of Formula (1), we found that a temperature increase of $24.5\text{ }^{\circ}\text{C}$ in the exhibition hall corresponds to the generation of 10.986 kWh of energy, and a temperature increase of $20\text{ }^{\circ}\text{C}$ in the storage room corresponds to the generation of 1.617 kWh of energy. That is to say, it requires 10.986 kWh of solar energy supply to meet the Thangka protection requirements in the exhibition hall at the lowest temperature throughout the year, and 1.617 kWh of solar energy supply to meet the Thangka protection requirements in the storage room. According to Figure 16, the heating demand in January is the highest throughout the year. According to Formula (7), the solar power generation E in the exhibition hall space must be guaranteed to be 7991 kWh to meet the requirements of indoor temperature, which is the minimum requirement. Through Equation (7) and Figure 6, the minimum installation area of solar panels for the Thangka exhibition hall is calculated to be 8.2 square meters. The heating demand in the Thangka storage room is 2582 kWh . The solar power generation E must be guaranteed to be at least 2582 kWh to meet the requirements of indoor temperature. The minimum installation area of the storage room solar panel is calculated to be 2.7 square meters. Through calculation, it is determined that at least 4.12% of the solar panels in the exhibition hall area and at least 1.88% of the solar panels in the storage room area need to operate throughout the year to maintain the temperature within the required range for both Thangka preservation and human thermal comfort.

Building upon this foundation, we investigated the robustness between temperature, energy consumption, and solar panels. The relationship between temperature and energy consumption is illustrated in Figure 17, showing a linear correlation where energy

consumption in both the exhibition hall and storage room uniformly increases with temperature. Additionally, since the optimal area of solar panels is calculated using Equation (7), which belongs to a standard linear equation, it indicates a linear relationship between solar irradiance, solar panel area, and energy consumption. This analysis contributes to the scientific rigor of the study.

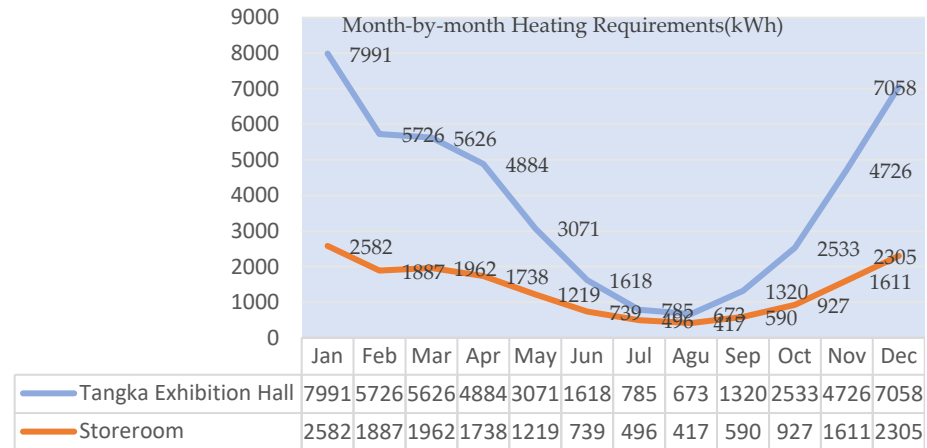


Figure 16. Month-by-month Heating Requirements.

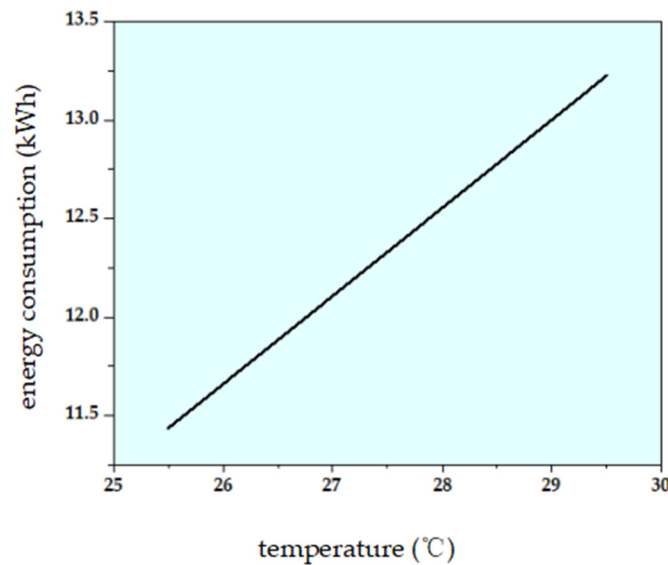


Figure 17. The relationship between temperature and energy consumption.

3 Thermal economy:

We have investigated materials with currently high photovoltaic conversion efficiency, as shown in Figure 5, which are priced at CNY 1500 per square meter. Calculations show that the installation areas for solar panels in the Thangka exhibition hall and the storage room are 8.2 square meters and 2.7 square meters, respectively. Consequently, the material costs for the exhibition hall and the storage room are calculated to be CNY 12,300 and CNY 4050, respectively. This indicates that the renovation of the Thangka exhibition hall requires at least CNY 12,300 to ensure that its indoor temperature meets the requirements for Thangka protection and human thermal comfort. Similarly, the Thangka storage room also requires at least CNY 4050 to ensure that the room temperature meets the requirements for Thangka preservation. The relatively low investment cost makes the design implementation economically viable and practical.

6. Conclusions

Utilizing renewable energy to reduce traditional energy consumption, decrease carbon emissions, and achieve optimal functionality and cost-effectiveness while simultaneously preserving heritage exhibition venues such as Thangka exhibition halls has become an effective approach to sustainable heritage conservation. This study takes a typical Thangka exhibition hall and its accompanying warehouse in southwestern China as an example to explore solutions for preserving Thangka using renewable energy. The research determined the optimal installation angle for solar panels to be 24.25 degrees, with an azimuth angle of -1.2 degrees. The optimal installation area for solar panels to meet near-zero energy consumption requirements for heating the building is 8.2 square meters, while for the storage room, it is 2.7 square meters. The area of solar panels required to meet Thangka protection temperature requirements accounts for approximately 4.12% of the area needed for near-zero energy consumption solar panels for heating, while for the storage room, it accounts for approximately 2.18%. This indicates that under the current conditions of the solar panel layout, the building can achieve heating with zero energy consumption and raise indoor temperatures to meet Thangka protection and human thermal comfort requirements, with minimal economic costs. Starting from the perspective of protecting intangible cultural heritage in minority rural areas, this study established a near-zero energy consumption solar system model, promoting the development of solar resource utilization in rural China.

This study represents an innovation in the utilization of solar energy by integrating rural environmental conditions, intangible cultural heritage preservation, and solar energy systems. It proposes an optimized practice of using renewable energy for architectural design to preserve heritage. However, this study serves merely as a case analysis of rural village buildings in western China, which has certain limitations. Future researchers could conduct more generalized studies based on this foundation. Despite these limitations, the study still provides guidance and a reference for promoting near-zero-energy buildings in rural areas.

Author Contributions: Conceptualization, W.H., Y.B. and Y.Z.; methodology, W.H. and Y.B.; software, Y.B. and W.H.; validation, Y.B., W.H. and Y.Z.; formal analysis, Q.Y. and Y.Z.; investigation, Y.B., M.D. and Y.T.; resources, W.H., Y.B. and Y.Z.; data curation, Q.Y. and Y.Z.; writing—original draft, W.H. and Y.B.; writing—review and editing, M.D., Q.Y. and Y.Z.; visualization, Q.Y., W.H. and Y.T.; supervision, Q.Y. and Y.Z. All authors have read and agreed to the published version of the manuscript.

Funding: This research was funded by the Chengdu Social Science Planning Project “Quantitative Research on the Construction of Park City Demonstration Area Based on Big Data under the Concept of Ecological Civilisation—Indicator System and Typical Cases” (Project No. 2021BS132). This research was funded by the Southwest Minzu University Graduate Innovative Research Project.

Data Availability Statement: The original contributions presented in the study are included in the article, further inquiries can be directed to the corresponding authors.

Conflicts of Interest: The authors declare no conflicts of interest. The funders had no role in the design of the study; in the collection, analyses, or interpretation of data; in the writing of the manuscript; or in the decision to publish the results.

References

1. Fei, J.; Han, D.; Ge, J.; Wang, X.; Koh, S.W.; Gao, S.; Sun, Z.; Wan, M.P.; Ng, B.F.; Cai, L. Switchable surface coating for bifunctional passive radiative cooling and solar heating. *Adv. Funct. Mater.* **2022**, *32*, 2203582. [[CrossRef](#)]
2. Dai, B.; Li, X.; Xu, T.; Zhang, X. Radiative cooling and solar heating janus films for personal thermal management. *ACS Appl. Mater. Interfaces* **2022**, *14*, 18877–18883. [[CrossRef](#)] [[PubMed](#)]
3. Pasupathi, M.K.; Alagar, K.; P, M.J.S.; M.M, M.; Aritra, G. Characterization of hybrid-nano/paraffin organic phase change material for thermal energy storage applications in solar thermal systems. *Energies* **2020**, *13*, 5079. [[CrossRef](#)]
4. Ansu, A.K.; Sharma, R.; Hagos, F.; Tripathi, D.; Tyagi, V. Improved thermal energy storage behavior of polyethylene glycol-based NEOPCM containing aluminum oxide nanoparticles for solar thermal applications. *J. Therm. Anal. Calorim.* **2021**, *143*, 1881–1892. [[CrossRef](#)]

5. Zheng, Z.; Chang, Z.; Xu, G.-K.; McBride, F.; Ho, A.; Zhuola, Z.; Michailidis, M.; Li, W.; Raval, R.; Akhtar, R. Microencapsulated phase change materials in solar-thermal conversion systems: Understanding geometry-dependent heating efficiency and system reliability. *ACS Nano* **2017**, *11*, 721–729. [[CrossRef](#)] [[PubMed](#)]
6. Tyagi, V.; Chopra, K.; Kalidasan, B.; Chauhan, A.; Stritih, U.; Anand, S.; Pandey, A.; Sari, A.; Kothari, R. Phase change material based advance solar thermal energy storage systems for building heating and cooling applications: A prospective research approach. *Sustain. Energy Technol. Assess.* **2021**, *47*, 101318. [[CrossRef](#)]
7. Li, X.; Sun, B.; Sui, C.; Nandi, A.; Fang, H.; Peng, Y.; Tan, G.; Hsu, P.-C. Integration of daytime radiative cooling and solar heating for year-round energy saving in buildings. *Nat. Commun.* **2020**, *11*, 6101. [[CrossRef](#)] [[PubMed](#)]
8. Hassan, H.; Abo-Elfadl, S.; El-Dosoky, M. An experimental investigation of the performance of new design of solar air heater (tubular). *Renew. Energy* **2020**, *151*, 1055–1066. [[CrossRef](#)]
9. Vengadesan, E.; Senthil, R. A review on recent development of thermal performance enhancement methods of flat plate solar water heater. *Solar Energy* **2020**, *206*, 935–961. [[CrossRef](#)]
10. Munusamy, A.; Barik, D.; Sharma, P.; Medhi, B.J.; Bora, B.J. Performance analysis of parabolic type solar water heater by using copper-dimpled tube with aluminum coating. *Environ. Sci. Pollut. Res.* **2023**, 1–16. [[CrossRef](#)]
11. Khimsuriya, Y.D.; Patel, D.; Said, Z.; Panchal, H.; Jaber, M.M.; Natrayan, L.; Patel, V.; El-Shafay, A. Artificially roughened solar air heating technology—A comprehensive review. *Appl. Therm. Eng.* **2022**, *214*, 118817. [[CrossRef](#)]
12. Kumar, P.G.; Balaji, K.; Sakthivadivel, D.; Vigneswaran, V.; Velraj, R.; Kim, S.C. Enhancement of heat transfer in a combined solar air heating and water heater system. *Energy* **2021**, *221*, 119805. [[CrossRef](#)]
13. Mayer, M.J.; Szilágyi, A.; Gróf, G. Environmental and economic multi-objective optimization of a household level hybrid renewable energy system by genetic algorithm. *Appl. Energy* **2020**, *269*, 115058. [[CrossRef](#)]
14. Zhang, Z.-Y.; He, Y.; Wang, Z.; Xu, J.; Xie, M.; Tao, P.; Ji, D.; Moth-Poulsen, K.; Li, T. Photochemical phase transitions enable coharvesting of photon energy and ambient heat for energetic molecular solar thermal batteries that upgrade thermal energy. *J. Am. Chem. Soc.* **2020**, *142*, 12256–12264. [[CrossRef](#)]
15. Abokersh, M.H.; Gangwar, S.; Spiekman, M.; Valles, M.; Jiménez, L.; Boer, D. Sustainability insights on emerging solar district heating technologies to boost the nearly zero energy building concept. *Renew. Energy* **2021**, *180*, 893–913. [[CrossRef](#)]
16. Dehghan, M.; Pfeiffer, C.F.; Rakhshani, E.; Bakhshi-Jafarabadi, R. A review on techno-economic assessment of solar water heating systems in the middle east. *Energies* **2021**, *14*, 4944. [[CrossRef](#)]
17. Koçak, B.; Fernandez, A.I.; Paksoy, H. Review on sensible thermal energy storage for industrial solar applications and sustainability aspects. *Solar Energy* **2020**, *209*, 135–169. [[CrossRef](#)]
18. Abokersh, M.H.; Valles, M.; Saikia, K.; Cabeza, L.F.; Boer, D. Techno-economic analysis of control strategies for heat pumps integrated into solar district heating systems. *J. Energy Storage* **2021**, *42*, 103011. [[CrossRef](#)]
19. Hosseini, S.M.; Carli, R.; Dotoli, M. Robust Optimal Demand Response of Energy-efficient Commercial Buildings. In Proceedings of the 2022 European Control Conference (ECC), London, UK, 12–15 July 2022; pp. 1–6.
20. Arteconi, A.; Ciarrocchi, E.; Pan, Q.; Carducci, F.; Comodi, G.; Polonara, F.; Wang, R. Thermal energy storage coupled with PV panels for demand side management of industrial building cooling loads. *Appl. Energy* **2017**, *185*, 1984–1993. [[CrossRef](#)]
21. Li, W.-T.; Tushar, W.; Yuen, C.; Ng, B.K.K.; Tai, S.; Chew, K.T. Energy efficiency improvement of solar water heating systems—An IoT based commissioning methodology. *Energy Build.* **2020**, *224*, 110231. [[CrossRef](#)]
22. Kalbasi, R.; Jahangiri, M.; Mosavi, A.; Dehshiri, S.J.H.; Dehshiri, S.S.H.; Ebrahimi, S.; Etezadi, Z.A.-S.; Karimipour, A. Finding the best station in Belgium to use residential-scale solar heating, one-year dynamic simulation with considering all system losses: Economic analysis of using ETSW. *Sustain. Energy Technol. Assess.* **2021**, *45*, 101097. [[CrossRef](#)]
23. Han, W.; Han, M.; Zhang, M.; Zhao, Y.; Xie, K.; Zhang, Y. Historic Building Renovation with Solar System towards Zero-Energy Consumption: Feasibility Analysis and Case Optimization Practice in China. *Sustainability* **2024**, *16*, 1298. [[CrossRef](#)]
24. Siraki, A.G.; Pillay, P. Study of optimum tilt angles for solar panels in different latitudes for urban applications. *Solar Energy* **2012**, *86*, 1920–1928. [[CrossRef](#)]
25. Sharma, M.K.; Kumar, D.; Dhundhara, S.; Gaur, D.; Verma, Y.P. Optimal tilt angle determination for PV panels using real time data acquisition. *Glob. Chall.* **2020**, *4*, 1900109. [[CrossRef](#)] [[PubMed](#)]
26. Schuster, C.S. The quest for the optimum angular-tilt of terrestrial solar panels or their angle-resolved annual insolation. *Renew. Energy* **2020**, *152*, 1186–1191. [[CrossRef](#)]
27. Zhong, Q.; Tong, D. Spatial layout optimization for solar photovoltaic (PV) panel installation. *Renew. Energy* **2020**, *150*, 1–11. [[CrossRef](#)]
28. Gardashov, R.; Eminov, M.; Kara, G.; Kara, E.G.E.; Mammadov, T.; Huseynova, X. The optimum daily direction of solar panels in the highlands, derived by an analytical method. *Renew. Sustain. Energy Rev.* **2020**, *120*, 109668. [[CrossRef](#)]
29. Meng, X.; Feng, R.; Yang, Y. Research status and development trend of solar heating technology. *IOP Conf. Ser. Earth Environ. Sci.* **2019**, *300*, 042081. [[CrossRef](#)]
30. Li, Z.; Wang, W. Study of image features between carved Thangka and embroidered Thangka. *J. Comput. Methods Sci. Eng.* **2021**, *21*, 367–381. [[CrossRef](#)]
31. Feng, F. Research on the Protection System of Thangka Intangible Cultural Heritage Based on VR Technology. *Acad. J. Sci. Technol.* **2023**, *7*, 178–182. [[CrossRef](#)]

32. Zhao, Y.; Zhou, L.; Liu, Z. Bibliometric Analysis of the Research Status of Thangka Images at Home and Abroad. *J. Phys. Conf. Ser.* **2020**, *1634*, 012108. [[CrossRef](#)]
33. Zhu, J. Research on the Conservation of Thangka. In Proceedings of the Second Academic Annual Conference of the Chinese Association for Cultural Heritage Conservation Technology, Xi'an, China, 1 July 2002.
34. Du, H.; Bai, Y. Research on the Cleaning of Ancient Thangka. In Proceedings of the Fourth Academic Annual Conference of the Chinese Association for Cultural Heritage Conservation Technology, Jingzhou, China, 7–11 November 2005; Science Press: Beijing, China, 2005; pp. 298–301.
35. Liu, H.; Tang, S.; Xie, H. Research on Thangka Image Restoration Technology Based on Sample Blocks. *Fujian Comput.* **2007**, *15–16*. [[CrossRef](#)]
36. *JGJ66-2015*; Code for Museum Building Design. MOHURD: Beijing, China, 2015.
37. *GB 50176-2016*; Code for Thermal Design of Civil Buildings. MOHURD: Beijing, China, 2017.
38. Za, S. A Brief Discussion on the Influence of Temperature, Humidity, and Environment on Thangka Preservation. *Sci. Wealth* **2019**, *12*. Available online: <https://www.fx361.cc/page/2019/1021/8186609.shtml> (accessed on 30 March 2024).
39. Xiu, D.; Zhang, X.; Xu, J.; Zhou, G.; Jiang, X.; Zhang, S.; Wang, J.; Hong, S. A novel porcelain-aluminum composite solar plate. *Shandong Sci.* **2021**, *34*, 68–76.
40. Tan, B. Storage Management of Thangka Cultural Relics. *Tibet. Sci. Technol.* **2008**, *6*, 15–17.

Disclaimer/Publisher's Note: The statements, opinions and data contained in all publications are solely those of the individual author(s) and contributor(s) and not of MDPI and/or the editor(s). MDPI and/or the editor(s) disclaim responsibility for any injury to people or property resulting from any ideas, methods, instructions or products referred to in the content.